Journal of Engineering Technology

Volume 8, Issue 2, July 2019, PP. 101-116

RESEARCH ARTICLE -ENGINEERNG TECHNOLOGY

3-D Geometrical Channel Model for Multipolarized ULA Massive MIMO Systems

Abdelhamid RIADI [1], Mohamed BOULOUIRD [1,2], MohaM'Rabet HASSANI [1]

[1]Instrumentation, Signals and Physical Systems (I2SP), Faculty of Sciences Semlalia, Cadi Ayyad University, Marrakech, Morocco.
[2]National School of Applied Sciences of Marrakech (ENSA-M), Cadi Ayyad University, Marrakech, Morocco

Abstract: This paper presents a novel method of three Dimensional (3D) channel design for multipolarized ULA-mMIMO (Uniform-Linear-Array-massive-Multiple-Input-Multiple-Output) systems using Spherical Wave (SW). Further, the proposed channel is estimated in UpLink (UL) transmission using Least Squares (LS).The main purpose of the paper is to reduce the channel orthogonality of the proposed method and ameliorate the system performance. In the same way the effect of Azimuth Angle of Arrival (AAoA), Elevation Angle of Arrival (EAoA), antenna spacing and cross-polarization discrimination (XPD) on the channel orthogonality are analyzed for the proposed method and compared with multipolarized ULA-mMIMO systems using Plane Wave (PW). The results demonstrate that the proposed multipolarized ULA-mMIMO systems using SWenhances the performance compared to multipolarized ULA-mMIMO using PW. The proposed method performs best under the analyzed parameters; while it's a best choice to realize a new configuration and improve the performance of massive-MIMO systems.

Keywords: Massive-MIMO, ULA, Multipolarized, unipolarized, channel orthogonality.

1 Introduction

Massive-MIMO system is a technology promising for the next generation 5G wireless communications. Nowadays, in a world of great mobility, the speed and capacity of communication systems are essential elements in order to keep people from all over the world in communication. Increasing the number of antennas at the Base Station (BS) and combined with OFDM (Orthogonal Frequency Division Multiplexing), massive MIMO can support very high throughput and/or performance of the links as well as spectral efficiency [1-38].

In other words, the channel orthogonality in massive-MIMO system is a term used to describe the favorable propagation between various terminals [2, 3, 4, 5]; further, to serve a various terminals with a feeble cross communication, the channel orthogonality must be low [6]; Thus it is advantageous for system performance. In a large antenna array, several works have appeared in recent years, investigate that the SW is considered, when the distance between the transceiver is shorter than Rayleigh distance, and the unipolarized ULA-mMIMO systems is used [7], [8] .

Otherwise, when the distance is high than Rayleigh distance the PW is satisfied [7], [8]; both the Azimuth Angle Spread/Elevation Angle Spread (AAS/EAS), some uniform distribution of AAS/EAS have been considered to characterize the AAoA/EAoA. Although, in massive-MIMO system the deployment of large antenna array in a narrow area leads to a high degree of risk (i.e., performance deterioration); thanks to a large spatial correlation between antennas [9]. So far, related to the literature, several work have been focused to investigate a real massive-MIMO system in a ULA configuration, with a same antenna spacing [10-12].Furthermore, in this paper our contributions are recapitulated as follows:

- ✓ a geometrical design is established for multipolarized ULA-mMIMO systems using SW;
- ✓ a 3-D channel is modeled basing on XPD, antenna spacing, AAoA and EAoA;
- ✓ a channel orthogonality is computed for our proposed method and compared with related work reference using PW.

This paper is organized as follows. In section 2, we illustrate the model of massive-MIMO system using higher order modulation 64-QAM and OFDM technique, in which the received signal is contaminated by an additive white gaussian noise (AWGN). In section 3, we introduce the LS channel estimation for a massive-MIMO array. Further, after getting the estimated channel, section 4 describes its behavior under various parameters. Moreover, in section 5, linear detector (i.e., Zero Forcing (ZF)) is discussed to illustrate the system performance. Section 6 presents the simulation results. Finally, we conclude this work in section 7.

2 Massive-MIMO system model

In this paper, we consider a massive-MIMO system in UL transmission from $\boldsymbol{N_t}$ terminals with single antenna to a single BS with $\boldsymbol{N_r}$ antennas. The considered system is presented in figure (1). It is a massive-MIMO-OFDM system with $\boldsymbol{N_r}$ and $\boldsymbol{N_t}$ receive and transmit antennas respectively. The length of sub-carriers and the cyclic prefix (CP) are defined by K and ν respectively. The CP is inserted on each terminal antenna to achieve a full OFDM symbol. In this paper, the CP is superior to the utmost multi-path delay [13-14-36].

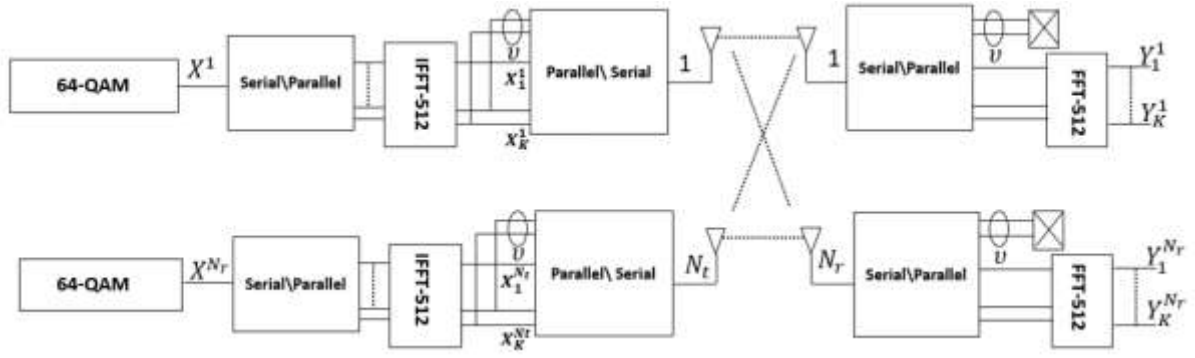

Figure. 1. System model.

In the same way, at the receiver the CP is removed on each BS antenna, taking for example the q^{th} BS antenna, the received signal vector $y^q(n)$ is $K \times 1$ and expressed as follow:

$$y^q(n) = \sum_{r=1}^{N_t} H_{cir}^{q,r} F^H X^r(n) + z^q(n) \quad (1)$$

From the equation (1), the circulant matrix $H_{cir}^{q,r}$ has a first column defined by $[h^{q,r^T}, 0_{1\times(K-L)}]^T$, in addition to that L is the length of the channel impulse response and $h^{q,r}$ present $L \times 1$ vector dimension. The OFDM vector that is transmitted on each terminal is defined by $X^r(n)$ with $K \times 1$ dimension, r and n are index of the number of terminal and time respectively, and $z^q(n)$ is an additive Gaussian noise at Time Index (TI) n, with zero mean and variance of σ_n^2. Moreover, the unitary DFT matrix with dimension $K \times K$ is presented by F; from the eigenvalue decomposition of the circulant matrix $H_{cir}^{q,r}$, it becomes $F^H diag\{\sqrt{K}F[h^{q,r^T}, 0_{1\times(K-L)}]^T\}F$ [14-37]. Finally, the FFT of the received signal $y^q(n)$ is given as follows$Y^q(n) = [Y_1^{q^T}(n), \cdots, Y_K^{q^T}(n)]^T$:

$$Y^q(n) = \sum_{r=1}^{N_t} diag\{\sqrt{K}F[h^{q,r^T}, 0_{1\times(K-L)}]^T\} \times X^r(n) + \Xi^q(n) \quad (2)$$

where $\Xi^q(n) = Fz^q(n)$.

3 Massive-MIMO Channel Estimation

Based on the same system presented in figure (1), the Least Square Channel Estimation (LSCE) scheme is presented. Then, the equation (2) can be written as:

$$Y^q(n) = \sum_{r=1}^{N_t} diag\{X^r(n)\}Fh^{q,r} + \Xi^q(n) \quad (3)$$

From the equation (3), F is $\sqrt{K} \times l$ of F, where l is the 1^{th} column of F. noting $X_{diag}^r(n) = diag\{X^r(n)\}$. Hence, the equation (3) becomes:

$$Y^q(n) = \sum_{r=1}^{Nt} X_{diag}^r(n)Fh^{q,r} + \Xi^q(n) \quad (4)$$

Furthermore, in this work the training of all OFDM symbols is done at maximum value g and the TI is $n \in \{0, \cdots, g-1\}$, we consider the data model:

$$Y^q = Ah^q + \Xi^q \quad (5)$$

where $Y^q = [Y^{q^T}(0), \cdots, Y^{q^T}(g-1)]^T$, $\Xi^q = [\Xi^{q^T}(0), \cdots, \Xi^{q^T}(g-1)]^T$

$$A = \begin{bmatrix} X_{diag}^1(0)F & \cdots & X_{diag}^{Nt}(0)F \\ \vdots & & \vdots \\ X_{diag}^1(g-1)F & \cdots & X_{diag}^{Nt}(g-1)F \end{bmatrix} \quad (6)$$

and $h^q = [h^{q,1^T}, \cdots, h^{q,Nt^T}]^T$. Basing on the cost function (equation 7); the LSCE technique minimizes the noise defined in equation (5) to finally obtain the estimated channel noted by $\hat{h}^q$

$$J(\hat{h}^q) = ||Y^q - A\hat{h}^q||^2 \quad (7)$$

$$= (Y^q - A\hat{h}^q)^H(Y^q - A\hat{h}^q)$$

$$= Y^{q^H}Y^q - Y^{q^H}A\hat{h}^q - \hat{h}^{q^H}A^HY^q + \hat{h}^{q^H}A^HA\hat{h}^q$$

In the next taking the derivation of the equation (7) relative to $\hat{h}^q$ variable,

$$\frac{\partial J(\hat{h}^q)}{\partial \hat{h}^q} = 2 * (-(A^H Y^q)^* + (A^H A\hat{h}^q)^*) = 0 \quad (8)$$

Finally, we have $A^H A\hat{h}^q = A^H Y^q$ and the solution of the LSCE is given by the following expression:

$$\hat{h}^q = A^+ Y^q \quad (9)$$

where A^+ is the pseudo-inverse that equals to $(A^H A)^{-1} A^H$ if $gK \geqslant LN_t$. Because $rank(A) = min(gK, LN_t)$, the necessary and sufficient condition to have unique LSCE is $gK \geqslant LN_t$. This LS method presents a low complexity and a high simplicity, in addition to that also taking the information about the channel and the noise are not necessary [14-34-35].

4 Channel modeling of Massive-MIMO system

In this paper, a new architecture is proposed as shown in figure (2), referring to a previous work [2], [7]. Moreover, in the case where the distance between the terminals and the BS antennas completely spaced (i.e., lengthy than the Rayleigh Distance (RD)), the PW is employed. While the distance between the terminals and BS antennas is smaller than RD, the SW is employed to characterize the channel. Based on the approach presented in section 3, the estimated channel $\widehat{H} \in \mathbb{C}^{N_r \times N_t}$ is noted by:

$$\widehat{H} = \begin{bmatrix} \hat{h}^{1,1} & \cdots & \hat{h}^{1,N_t} \\ \vdots & & \vdots \\ \hat{h}^{q,1} & \cdots & \hat{h}^{q,N_t} \\ \vdots & & \vdots \\ \hat{h}^{N_r,1} & \cdots & \hat{h}^{N_r,N_t} \end{bmatrix} = [\hat{h}_1, \dots, \hat{h}_e, \dots, \hat{h}_f, \dots, \hat{h}_{N_t}] \quad (10)$$

Moreover the channel orthogonality (i.e., favorable propagation) between different terminals can be noted by [4], [17]:

$$\delta_{e,f} = \frac{|(\hat{h}_e)^H \hat{h}_f|}{||\hat{h}_e||.||\hat{h}_f||} \quad (11)$$

where $||.||$ signify the Euclidean norm and $\hat{h}_i = [\hat{h}^{1,i^T}, \cdots, \hat{h}^{N_r,i^T}]^T$, $i = (e, f)$ is a channel vector of the i^{th} terminal and$\hat{h}^{1,i^T}$ is the path from thei^{th} terminal tothe first antenna of the BS. Furthermore, the purpose of this paper is to consider the 3D multipolarized ULA-mMIMO systems (figure(2)), all pair antennas are vertically polarized and all odd antennas are horizontally polarized, in addition to that the SW is considered and the paths arrive from S with randomly angles for all antennas with AAoA α and EAoA β, S' is the projection of S on x-S_1-y and h is the height of S. Although, d_x and d_y are the projection of the S' on x axis and y axis respectively. The neighboring antenna distance is noted by d. From the figure (2), theright triangles $SS'S_1$, …, $SS'S_{N_r}$have a right angle S'. Basing on Pythagorean theorem. The distances between the source S and each antenna element are defined as follows:

$$d_{SS_1} = \sqrt{d_x^2 + d_y^2 + h^2} \quad (12)$$

$$d_{SS_2} = \sqrt{(d_x + d)^2 + d_y^2 + h^2} \quad (13)$$

⋮

$$d_{SS_m} = \sqrt{(d_x + d(m-1))^2 + d_y^2 + h^2} \quad (14)$$

$$\vdots$$

$$d_{SS_{N_r}} = \sqrt{(d_x + d(N_r - 1))^2 + d_y^2 + h^2} \quad (15)$$

In the same way, for the different angles$\angle yS_iS'$isα_i and$\angle SS_iS'$isβ_i, $\forall i \in \{1, \cdots, N_r\}$,$d_x$ and h can be denoted by:

$$d_x = tan(\alpha_i) \times d_y - d(i-1) \quad (16)$$

$$h = tan(\beta_i)\sqrt{tan^2(\alpha_i) \times d_y^2 + d_y^2} \quad (17)$$

From our proposed schema (figure (2)), the AAS and EAS are used to characterize the AAOA and EAOA distributions. Hence, based on the uniform distribution presented in [2], the Power Azimuth Spread (PAS) of AAS/EAS is described as follows [2], [18]:

$$p(\mathrm{Y}) = \frac{1}{2\Delta \mathrm{Y}}, \quad -\Delta \mathrm{Y} + \mathrm{Y}_0 \leqslant \mathrm{Y} \leqslant \Delta \mathrm{Y} + \mathrm{Y}_0, \quad (18)$$

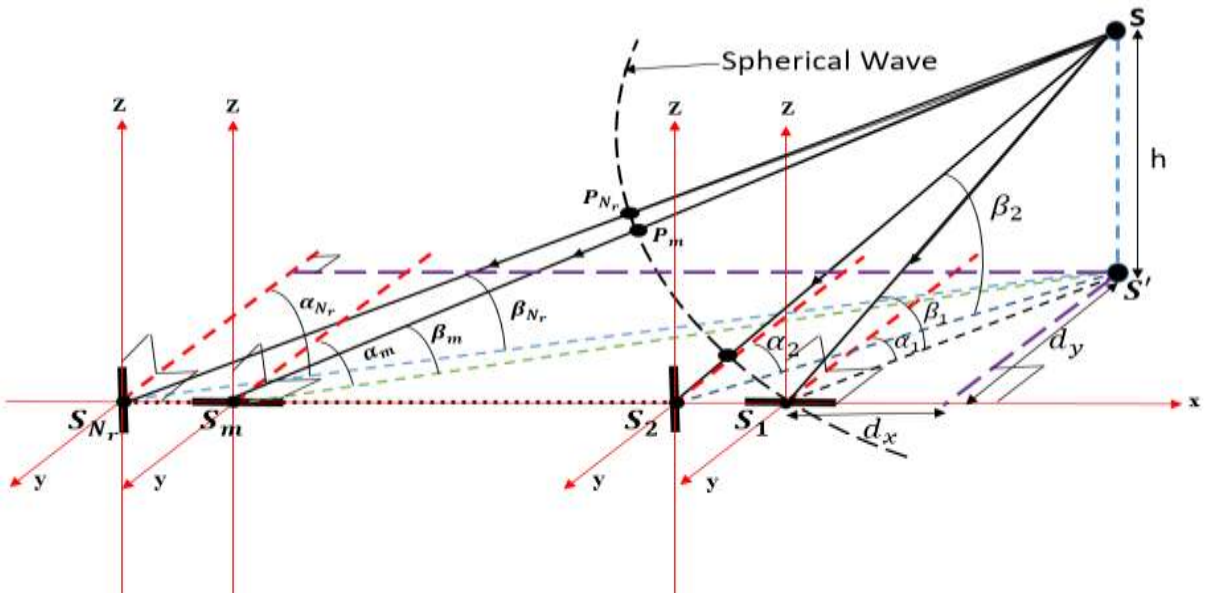

Figure. 2. 3D multipolarized uniform linear array massive-MIMO

In the same way, the ΔY presents the AAS/EAS, where the Y_0 is the mean of AAoA/EAoA. According to previous equations (12, 13,…, 15) and respecting antenna S_1 as a reference antenna of the system. Two estimated paths is defined at antennasS_1 and S_2 by the following expressions:

$$\hat{h}_1^{ULA} = \sqrt{P_H} e^{j(\phi + 2\pi\sqrt{d_x^2 + d_y^2 + h^2}/\lambda)} \quad (19)$$

$$\hat{h}_2^{ULA} = \sqrt{P_V} e^{j(\phi + 2\pi\sqrt{(d_x+d)^2+d_y^2+h^2}/\lambda)} \quad (20)$$

Where λ is a wavelength, and ϕ is uniform random phase component Independent and Identically Distributed (IID) on $[-\pi, \pi)$. In the same way P_H and P_V are horizontally and vertically polarized power [2], [19]. Accordingly, the channel vectors at terminal location e with single horizontally polarized antenna and f with single vertically polarized antenna can be written by:

$$\hat{h}_e^{ULA,XPD} = \begin{bmatrix} \hat{h}_{ULA,XPD}^{1,e} \\ \hat{h}_{ULA,XPD}^{2,e} \\ \vdots \\ \hat{h}_{ULA,XPD}^{m,e} \\ \vdots \\ \hat{h}_{ULA,XPD}^{N_r,e} \end{bmatrix} = \begin{bmatrix} \sqrt{P_H a} e^{j(\phi_e + 2\pi\sqrt{d_{x,e}^2+d_{y,e}^2+h_e^2}/\lambda)} \\ \sqrt{P_H(1-a)} e^{j(\phi_e + 2\pi\sqrt{(d_{x,e}+d)^2+d_{y,e}^2+h_e^2}/\lambda)} \\ \vdots \\ \sqrt{P_H(1-a)} e^{j(\phi_e + 2\pi\sqrt{(d_{x,e}+d(m-1))^2+d_{y,e}^2+h_e^2}/\lambda)} \\ \vdots \\ \sqrt{P_H(1-a)} e^{j(\phi_e + 2\pi\sqrt{(d_{x,e}+d(N_r-1))^2+d_{y,e}^2+h_e^2}/\lambda)} \end{bmatrix}, \quad (21)$$

$$\hat{h}_f^{ULA,XPD} = \begin{bmatrix} \hat{h}_{ULA,XPD}^{1,f} \\ \hat{h}_{ULA,XPD}^{2,f} \\ \vdots \\ \hat{h}_{ULA,XPD}^{m,f} \\ \vdots \\ \hat{h}_{ULA,XPD}^{N_r,f} \end{bmatrix} = \begin{bmatrix} \sqrt{P_V(1-a)} e^{j(\phi_f + 2\pi\sqrt{d_{x,f}^2+d_{y,f}^2+h_f^2}/\lambda)} \\ \sqrt{P_V a} e^{j(\phi_f + 2\pi\sqrt{(d_{x,f}+d)^2+d_{y,f}^2+h_f^2}/\lambda)} \\ \vdots \\ \sqrt{P_V a} e^{j(\phi_f + 2\pi\sqrt{(d_{x,f}+d(m-1))^2+d_{y,f}^2+h_f^2}/\lambda)} \\ \vdots \\ \sqrt{P_V a} e^{j(\phi_f + 2\pi\sqrt{(d_{x,f}+d(N_r-1))^2+d_{y,f}^2+h_f^2}/\lambda)} \end{bmatrix}. \quad (22)$$

For visual representation of the horizontally and vertically polarized phenomena in real environment; the horizontal or vertical polarization at terminal ordinary location can be changed at BS antennas by vertical or horizontal polarization, naturally due to multipath phenomena (i.e., diffusions, reflections, refractions and diffractions, ...). Hence, to model these phenomena is to establish the cross-polarization discrimination (XPD) [2], [20]:

$$XPD = \frac{E\{|h_{VV}|^2\}}{E\{|h_{VH}|^2\}} = \frac{E\{|h_{HH}|^2\}}{E\{|h_{HV}|^2\}} = \frac{1-a}{a}, \quad (23)$$

From the equation (23), $E\{\}$ illustrates the expectation operator, the h_{VV} and h_{HH} are the co-polarized channels both vertically and horizontally polarized antenna respectively, the cross-polarized channels are given by h_{VH} and h_{HV} for vertically/horizontally and horizontally/vertically polarized antennas respectively. In the same way, a is the power escaped from horizontal to vertical polarization and inversely [2], [21-24]. Moreover, in the case there is no escape a equals to 0. Whereas, there is escape a is $0 < a \leq 1$. Hence, one estimated path channel of multipolarized ULA-mMIMO comprising XPD phenomenon can be writing as:

$$\hat{h}_1^{ULA} = \sqrt{P_H a + P_V(1-a)} e^{j(\phi + 2\pi\sqrt{d_x^2+d_y^2+h^2}/\lambda)} \quad (24)$$

$$\hat{h}_m^{ULA} = \sqrt{P_V a + P_H(1-a)} e^{j(\phi + 2\pi\sqrt{(d_x+d(m-1))^2+d_y^2+h^2}/\lambda)} \quad (25)$$

In this way, at receive antenna the XPD has an impact on the receiving power, when the polarization is the same both the transceiver, the power is modeled by $P_x(1-a)$, $x \in (V,H)$. Otherwise, when the polarization is differently both the transceiver, the power is modeled by $P_x a$, $x \in (V,H)$ [2], [25].In this paper, we compare our proposed architecture with the 3-D multipolarized ULA-mMIMO systems as defined in [1]. From this work the channel orthogonality can be defined by the same equation (11) for the two estimated channel vectors expressed by [2]:

$$\hat{h}_{\square}^{\square\square\square,\square\square\square} = \begin{bmatrix} \hat{h}_{\square\square\square,\square\square\square}^{1,\square} \\ \hat{h}_{\square\square\square,\square\square\square}^{2,\square} \\ \vdots \\ \hat{h}_{\square\square\square,\square\square\square}^{\square,\square} \\ \vdots \\ \hat{h}_{\square\square\square,\square\square\square}^{\square_{\square}-1,\square} \\ \hat{h}_{\square\square\square,\square\square\square}^{\square_{\square},\square} \end{bmatrix} = \begin{bmatrix} \sqrt{\square_{\square}\square_{\square}}\,\square^{\square(\square_{\square})} \\ \sqrt{\square_{\square}(1-\square_{\square})}\,\square^{\square(\square_{\square}+2\square\square\square\square(\frac{\square}{2}-\square_{\square})\square\square\square(\square_{\square})/\square)} \\ \vdots \\ \sqrt{\square_{\square}(1-\square_{\square})}\,\square^{\square(\square_{\square}+2\square\square(\square-1)\square\square\square(\frac{\square}{2}-\square_{\square})\square\square\square(\square_{\square})/\square)} \\ \vdots \\ \sqrt{\square_{\square}\square_{\square}}\,\square^{\square(\square_{\square}+2\square\square(\square_{\square_{\square}-1}-1)\square\square\square(\frac{\square}{2}-\square_{\square})\square\square\square(\square_{\square})/\square)} \\ \sqrt{\square_{\square}(1-\square_{\square})}\,\square^{\square(\square_{\square}+2\square\square(\square_{\square}-1)\square\square\square(\frac{\square}{2}-\square_{\square})\square\square\square(\square_{\square})/\square)} \end{bmatrix}, \quad (28)$$

$$\hat{h}_{\square}^{\square\square\square,\square\square\square} = \begin{bmatrix} \hat{h}_{\square\square\square,\square\square\square}^{1,\square} \\ \hat{h}_{\square\square\square,\square\square\square}^{2,\square} \\ \vdots \\ \hat{h}_{\square\square\square,\square\square\square}^{\square,\square} \\ \vdots \\ \hat{h}_{\square\square\square,\square\square\square}^{\square_{\square}-1,\square} \\ \hat{h}_{\square\square\square,\square\square\square}^{\square_{\square},\square} \end{bmatrix} = \begin{bmatrix} \sqrt{\square_{\square}(1-\square_{\square})}\,\square^{\square(\square_{\square})} \\ \sqrt{\square_{\square}\square_{\square}}\,\square^{\square(\square_{\square}+2\square\square\square\square(\frac{\square}{2}-\square_{\square})\square\square\square(\square_{\square})/\square)} \\ \vdots \\ \sqrt{\square_{\square}\square_{\square}}\,\square^{\square(\square_{\square}+2\square\square(\square-1)\square\square\square(\frac{\square}{2}-\square_{\square})\square\square\square(\square_{\square})/\square)} \\ \vdots \\ \sqrt{\square_{\square}(1-\square_{\square})}\,\square^{\square(\square_{\square}+2\square\square(\square_{\square_{\square}-1}-1)\square\square\square(\frac{\square}{2}-\square_{\square})\square\square\square(\square_{\square})/\square)} \\ \sqrt{\square_{\square}\square_{\square}}\,\square^{\square(\square_{\square}+2\square\square(\square_{\square}-1)\square\square\square(\frac{\square}{2}-\square_{\square})\square\square\square(\square_{\square})/\square)} \end{bmatrix}. \quad (29)$$

5 Linear Detector

In this section, the ZF detector is presented, after getting the channel estimation in the UL transmission for $\square_{\square}$ single antenna terminals defining as

$$\hat{\square} = [\hat{h}_1^{\square\square\square,\square\square\square}, \cdots, \hat{h}_{\square}^{\square\square\square,\square\square\square}, \cdots, \hat{h}_{\square}^{\square\square\square,\square\square\square}, \cdots, \hat{h}_{\square_{\square}}^{\square\square\square,\square\square\square}] \quad (30)$$

for multipolarized ULA-mMIMO systems. In this paper and in related references [2], [26], it was supposed that the number of terminals with vertically polarized antenna are equal to the number of terminals with horizontally polarized antenna due to arbitrary location. In order to detect the data, we proceed to the technique defined in [27]. Hence, the linear MIMO detectors are based on a linear transformation of the received signal vector y (Figure 3):

$$\square = \square\square \quad (31)$$

Where $\square$ is the linear transformation matrix designed using various criteria [27], [33-34] and $\square = [\square^{1}, \ldots, \square^{\square}, \ldots, \square^{\square_{\square}}]^{\square}$. A conceptual illustration of MIMO linear detector is given in Figure (3). The data detected after passing through the 64-QAM demodulator is given by $\hat{\square}$.

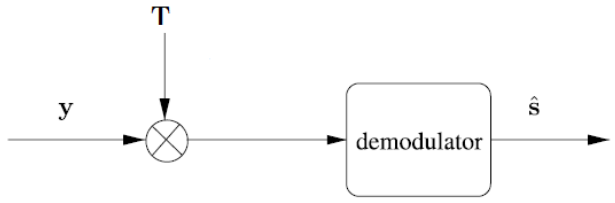

Figure. 3. Conceptual illustration of linear MIMO detectors.

The ZF is a linear detection scheme which forces the interference to zero. However, it can result in an increase in the noise level [1], [27-28] and [33-34]. According to equation (30) the linear transformation matrix is given by:

$$□_{□□} = \hat{□}^{+} \tag{32}$$

where $\hat{□}^{+} = (\hat{□}^{□}\hat{□})^{-1}\hat{□}^{□}$, the matrix $\hat{□}$ satisfies $□_{□} > □_{□}$ and a complete column rank of $□_{□}$.

6 Simulation Results

In this section, we present a collection of performance results; firstly the channel orthogonality for multipolarized/unipolarized massive-MIMO system with various parameters. Secondly after getting the channel estimation we use the linear detector ZF to elaborate the performance of multiplarized/unipolarized ULA-mMIMO for PW and SW, in which we evaluate their performances in terms of Bit Error Rate(BER). In this part, we assume channels with L=1 taps. These taps are simulated as IID. The length of OFDM subcarriers (i.e., OFDM symbol), that is transmitted from each terminal antenna equals to $□ = 512$ and the CP of length $□ = 128$, the pilot tones dedicated for training of length $\frac{□}{2}$ are equipowered and equispaced. This on the one hand, on the other hand the length of sequence data is also equals to $\frac{□}{2}$. Hence, using the Monte Carlo simulation to generate 10000 realizations of channel and $□ = 100$ consecutive OFDM symbols.

Figure (4) presents different curves of channel orthogonality both multipolarized/unipolarized ULA-mMIMO with SW/PW, the antenna spacing is equal $0.5□$, mostly used in massive-MIMO systems [6], [29-31], the power is normalized and the XPD=8 dB according to [2], [32]; in the same way the mean of AAoA/EAoA is set to be $0^{□}$. Furthermore, when the number of antennas increases the channel orthogonality decreases. Both a poor scattering (i.e., $□□□ = 3^{□}$) and a large scattering (i.e., $□□□ = 30^{□}$) the channel orthogonality decreases when the BS antennas increase. In the case when the number of antennas equals 20 and the $□□□ = 3^{□}$ the channel orthogonality is nearly 0.36 for multipolarized PW, while it is nearly 0.13 for multipolarized SW. In addition to that the channel orthogonality using multiploarized PW is smaller than unipolarized SW when the AAS equals to $30^{□}$ and performs like multipolarized SW with a poor AAS. Accordingly, from the table 1, in a poor scatteringand a high BS antenna (i.e., $□_{□}$ =200) the proposed multipolarized ULA-mMIMOdecreses more the channel orthogonality at a value equals 0.04, compared to multipolarized ULA-mMIMO using PW with value equals 0.12. From this results with a small AAS, the multipolarized ULA-mMIMO using SW can reduce the demand of rich scattering compared with ULA-mMIMO using PW anda classical MIMO, that on the one hand.

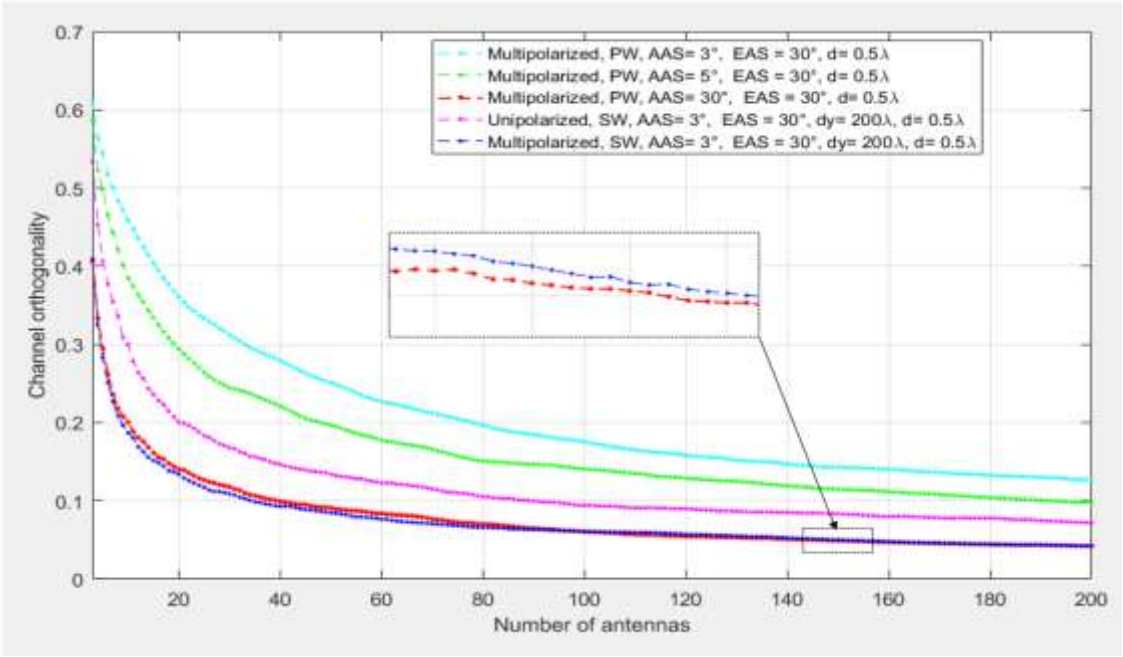

Figure. 4. Channel orthogonality vs number of antennas for different AAS.

Table 1. Comparative results of channel orthogonality both SW and PW for multipolarized antennas

	AAS = 3°,	EAS = 30°
	SW	PW
N_t	Multipolarized	Multipolarized
20	0.13	0.36
100	0.06	0.17
200	0.04	0.12

In the other hand, figure (5) shows the channel orthogonality curves for various antenna spacing, AAS is equal to 3° and EAS is equal to 30°. These results describe for the first time an increasing of channel orthogonality over the range of BS antennas. When the BS antennas is set to be 20 the channel orthogonality are nearly 0.5 and 0.22 for unipolarized PW with an antenna spacing equals0.2λ and 2λ respectively; in addition to that the channel orthogonality is closely 0.2 for unipolarized SW with $d_y = 2\lambda$; for multipolarized antennas array, with an antenna spacing equals2λ the channel orthogonality are closely 0.16 and 0.13 for PW and SW respectively (Table 2). Hence, with a few BS antennas the spacious antenna spacing has important benefit; in the same way multipolarized ULA-mMIMO using SW has a high advantage to decline the channel orthogonality to a lower value, compared to multipolarized ULA-mMIMO using PW (Table 2). Moreover, with a large antennas array (i.e., $N_t = 200$) the channel orthogonality decreases more and is closely to 0.04 despite the antenna spacing is set to be 2λ with multipolarized antenna array using SW. Furthermore with an antenna spacing equals to 0.5λ (figure (4) and Table 2) the channel orthogonality is closely to 0.04 with a large BS antennas (i.e., $N_t = 200$) ; while the channel orthogonality of multipolarized

using PW nearly 0.05 with d=2□ and 0.1 with d=0.5□ (Table 2). Hence, multipolarized SW with a large antenna array can reduce the demand for spacious antenna spacing under a poor scattering; and declines more the channel orthogonality (i.e., favorable propagation) compared to multipolarized ULA-mMIMO using PW.

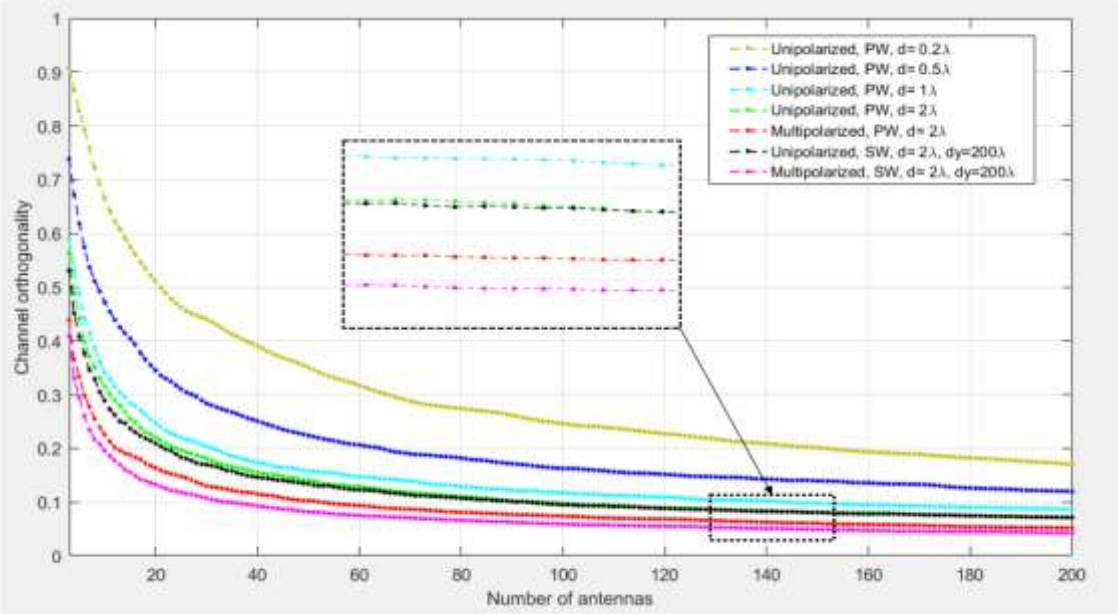

Figure. 5. Channel orthogonality vs number of antennas for different antenna spacing.

Table 2. Channel orthogonality both SW and PW for multipolarized antennas with a high and low antenna spacing

	SW-Multipolarized		PW- Multipolarized	
□□	d = *0.5*	d = *2*	d = 0.5	d = *2*
20	0.1342	0.1327	0.3609	0.1633
100	0.06077	0.05923	0.1753	0.07394
200	0.0428	0.04267	0.1263	0.05175

Otherwise, figure (6) presents various curves of channel orthogonality with different XPD, in this case the □□□ = 3□ and □□□ = 30□, the channel orthogonality is equally sensitive to XPD for multipolarized PW and SW ULA-mMIMO systems, the antenna spacing is set to be 0.5□. This figure shows a decreasing of channel orthogonality both multipolarized PW and SW. For a few antennas array as 20 the channel orthogonality are closely 0.7 and 0.18 with a XPD=0 dB both multipolarized PW and SW respectively (Table 3), in the same way when the XPD is set to be 15 dB the channel orthogonality are closely 0.35 and 0.1 both multipolarized PW and SW respectively. furthermore, when the BS antennas array increase (i.e., □□ = *200*) the channel orthogonality decreasesto 0.03 and 0.14 both multipolarized SW and PW respectively. Accordingly, increasing the nomber of antennas at the BS, the channel orthogonality both multipolarized ULA-mMIMO using SW and PW decreases; while the proposed method using SW performs more than multipolarized ULA-mMIMO usingPW

(Table 3). Hence, these results show a great benefit of multipolarized ULA-mMIMO systems using SW to decline the channel orthogonality, when a small and higher power leakage is used.

In the next of this paper, the performance of multipolarized/unipolarized ULA-mMIMOusing PW/SW are discussed basing on ZF detector. The XPD is set to be 8 dB and the antenna spacing equals to 0.5□, similarity the □□□ = 3^o and the □□□ = $30^□$. From the figure (7), the estimated channels using PW and SW are used such as $\hat{□}^{□□}$ = [$\hat{□}_1^{□□□,□□□,□□}$, ⋯, $\hat{□}_{□□}^{□□□,□□□,□□}$] and $\hat{□}^{□□}$ = [$\hat{□}_1^{□□□,□□□,□□}$, ⋯, $\hat{□}_{□□}^{□□□,□□□,□□}$].In addition to that the number of terminals is equal to 8 and the BS antennas array is set to be 200. The BER decreases as the BS antennas array increase, and it seems that the BER is the same of channel orthogonality. We note in a range of a small Signal to Noise Ratio(SNR) the unipolarized SW performs more than unipolarized PW; similarly multipolarized SW performs more than multipolarized PW. Otherwise the same remark with a higher SNR. The gaps between the true channel using multipolarized and unipolarized ULA-mMIMO antennas array using PW is 7.23 dB, also equals to 5.33 against unipolarized ULA-mMIMOusing SW, in addition to that are equal to 3.16 and 0.37 for Multipolarized antennas array using PW and SW respectively, for a □□□ = 21.98×10^{-5} .

Consequently in a poor scattering communication environment, and under the considered method (section 4), a significant power leakage between transceiver and antenna spacing is used; the multipolarized ULA-mMIMO using SW in our proposed architecture (figure (2)) out performs multipolarized ULA-mMIMO systems using PW presented in [*2*].

Similarely, From the table 4 the BER is sensitive to the SNR, a large SNR results in alower BER. When the SNR is -6 dB and the total number of transferred bits is equal to 10^5, thenumber of bit errors are nearly 4763 and 5310 for unipolarized SW and PW respectively; at a SNR equals to 6 dB the number of bit errors drop to844 and 1086 for unipolarized SW and PW respectively; and with multipolarized ULA-mMIMO systems, the number of bit errors are nearly 3532 and 4763 using SW and PW respectively with the total number of transferred bits is equal to $10^5$and the SNR becomes -6 dB; in addition to that the number of bit errors dropped to38 and 244 for SW and PW respectively with a SNR equals to 6 dB. Consequently, we require a noticeable reduction in confidence levelof bit errorsfrom92.07% to 2.17%(i.e., increasing the probability of bits without errors from 7.93% to 97.83%)with true channel, and from97.08% to 3.77% with multipolarized antenna using SW; while for multipolarized antenna using PW offers a reduction from 99.15% to 21.69% . Otherwise, for unipolarized antenna using SW the confidence level of bit errors is dropped from 99.15% to 57.0142%; in addition to that the unipolarized antenna using PW offers a reduction from 99.51% to 66.244% for a -6 dB ≤ SNR ≤ 6dB.Thereby, the proposed method performs best compared to ULA-mMIMO using PW.

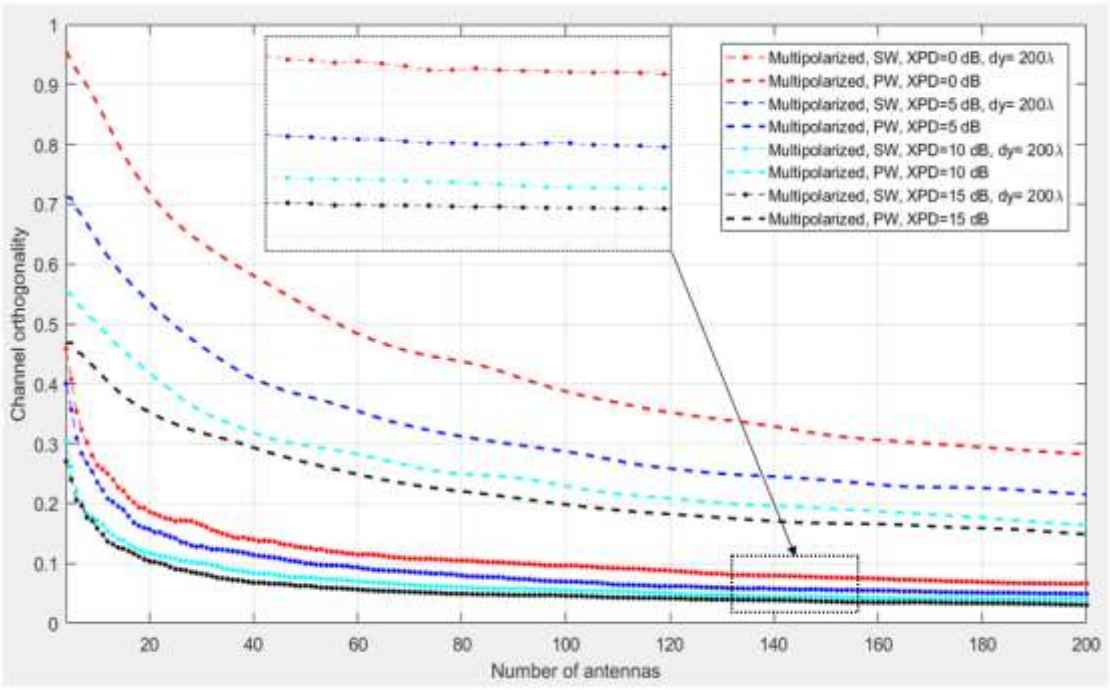

Figure. 6. Channel orthogonality vs number of antennas for different cross-polarization discrimination.

Table 3. Channel orthogonality both SW and PW for multipolarizedwithvarious XPD

	SW-Multipolarized		PW- Multipolarized	
XPD (dB)	□□ = *20*	□□ = *200*	□□ = *20*	□□ = *200*
0	0.186	0.06609	0.7195	0.2818
5	0.1569	0.04884	0.537	0.2147
15	0.1033	0.03038	0.3525	0.1483

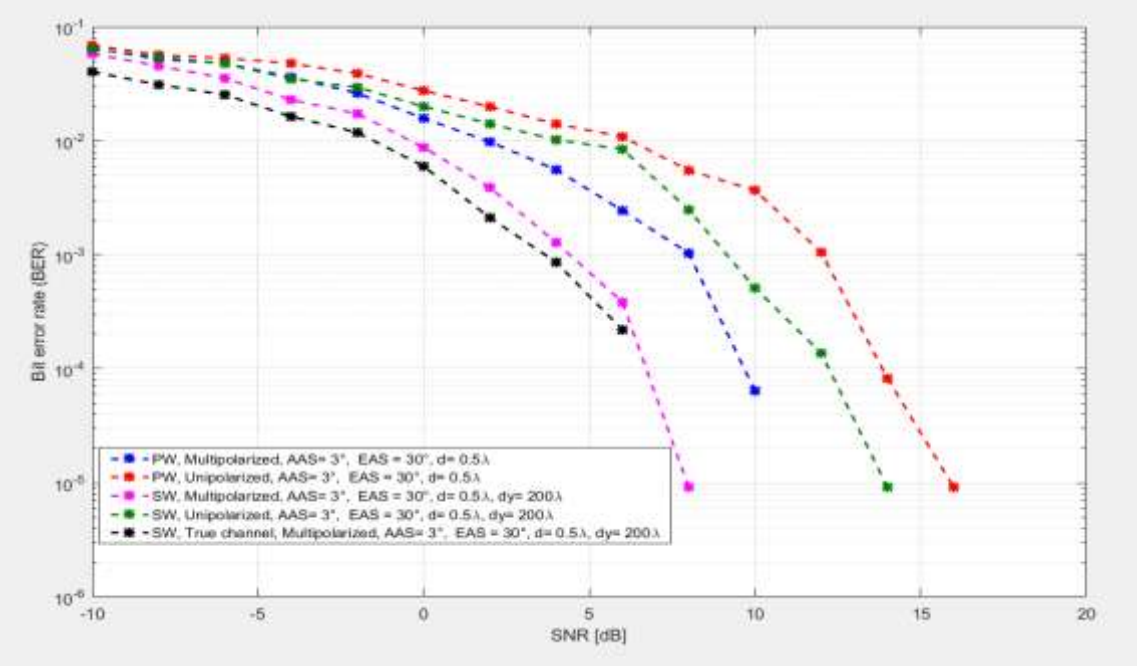

Figure. 7. Bit Error Rate vs Signal to Noise Ratio using Zero Forcing detector.

Table 4. Bit Error Rate both SW and PW for multipolarized/unipolarized ULA-mMIMO

	BER				
	SW			PW	
SNR (dB)	True channel	Multipolarized	Unipolarized	Multipolarized	Unipolarized
-6	2534×10^{-5}	3532×10^{-5}	4763×10^{-5}	4763×10^{-5}	5310×10^{-5}
0	598×10^{-5}	875.5×10^{-5}	2000×10^{-5}	1570×10^{-5}	2755×10^{-5}
6	21.98×10^{-5}	38.46×10^{-5}	844.3×10^{-5}	244.5×10^{-5}	1086×10^{-5}

7 Conclusion

This study has shown a communication system in uplink transmission for an ULA-mMIMO design. The PW and SW effect are investigated; from the outcome of our investigation, it is possible to conclude that multipolarized antennas array basing on SW has a benefit advantage to decrease the channel orthogonality.Moreover, the estimated channel with multipolarized ULA-mMIMO systems exhibits a noticeable enhancement of the probability of bits without errors from 2.92% to 96.23%, and outperforms the estimated channel of multipolarized antenna using PW with an enhancement from 0.85% to 78.31%. While the enhancement of the estimated channel with unipolarized ULA-mMIMO using SW is from 0.85% to 42.99%, outperforms the estimated channel of unipolarized antenna using PW with an enhancement from 0.49% to 33.76%. The results obtained indicate that proposed multipolarized ULA-mMIMO performs approximately like the true channel with an enhancement from 7.93% to 97.83%;it also enhances the system performance compared to

multipolarized/unipolarized ULA-mMIMOantennas using PW. Summing up the results, it can be concluded that our proposed 3-D channel with a large antennas array can take down shorthand a large antenna spacing that on the one hand. On the other, the demand of rich scattering and high escaped power are declined. Consequently, the proposedmultipolarized ULA-mMIMO method can be readily used in practice according to a small scale parameters considered.

References

[1]. Prajapati Rajeev, Adhikari Prabhat, and Lama Norsang, "Sphere detection technique: An optimum detection scheme for mimo system", *International Journal of Computer Applications*, Vol. 100, No. 2, 2014.

[2]. Xudong Cheng, Yejun He, Li Zhang and Jian Qiao, "Channel modeling and analysis for multipolarized Massive MIMO systems", *International Journal of Communication Systems*, Vol.31, No.12, pp. 3703, 2018.

[3]. Trinh Van Chien and Emil Bjornson, "Massive MIMO Communications", *5G Mobile Communications*, pp 77-116, 2017.

[4] K. Zheng, S. Ou and X. Yin, "Massive MIMO channel models: A survey",*International Journal of Antennas and Propagation*, vol. 11, pp. 1-10, 2014.

[5]. Wu X, Beaulieu NC, Liu D. "On favorable propagation in massive MIMO systems and different antenna configurations", *IEEE Access*.Vol. 5, pp.5578-5593, 2017.

[6]. J. Hoydis, C. Hoek, T. Wild and S. ten Brink, "Channel measurements for large antenna arrays",*Proc. 2012 International Symposium on Wireless Communication Systems (ISWCS)*, pp. 811-815, 2012.

[7]. Cheng, Xudong and He, Yejun, "Channel Modeling and Analysis of ULA Massive MIMO Systems", *2018 20th International Conference on Advanced Communication Technology (ICACT)*, pp. 411-416, 2018.

[8]. Liu Liu, David W. Matolak, Cheng Tao, Yongzhi Li, Bo Ai and Houjin Chen, "Channel capacity investigation of a linear massive MIMO system using spherical wave model in LOS scenarios", *Science China Information Sciences*, vol. 59, No. 2, pp. 1-15, 2016.

[9]. Jaehyun Park and Bruno Clerckx, "Multi-User Linear Precoding for Multi-Polarized Massive MIMO System Under Imperfect CSIT", *IEEE Transactions on Wireless Communications*, vol. 14, No. 5, pp. 2532-2547, May 2015.

[10]. X. Gao, F. Tufvesson, O. Edfors and F. Rusek, "Measured propagation characteristics for very-large MIMO at 2.6 GHz",*Proc. 2012 Conference Record of the Forty Sixth Asilomar Conference on Signals, Systems and Computers (ASILOMAR)*, pp. 295-299, Nov. 2012,

[11]. X. Gao, O. Edfors, F. Rusek and F. Tufvesson, "Massive MIMO Performance Evaluation Based on Measured Propagation Data", *IEEE Transactions on Wireless Communications*, vol. 14, No. 7, pp. 3899-3911, Mar. 2015.

[12]. M. Gauger, J. Hoydis, C. Hoek, H. Schlesinger, A. Pascht and S. ten Brink, "Channel Measurements with Different Antenna Array Geometries for Massive MIMO Systems", *Proc. 2015 10th International ITG Conference on Systems, Communications and Coding (SCC)*, pp. 1-6, Feb. 2015.

[13]. Moradi, Alieh and Bakhshi, Hamidreza and Najafpoor, Vahid, "Pilot Placement for Time-Varying MIMO OFDM Channels with Virtual Subcarriers", *Communications and Network*, Vol.3, No.1, pp. 31, 2011.

[14]. Barhumi, Imad and Leus, Geert and Moonen, Marc, "Optimal training design for MIMO OFDM systems in mobile wireless channels", *IEEE Transactions on signal processing*, Vol. 51, No. 6, pp. 1615-1624, 2003.

[15]. Cantrell, Cyrus D, "Modern mathematical methods for physicists and engineers", *Cambridge University Press*, 2000.

[16]. Tung, Tai-Lai and Yao, Kung and Hudson, RE, "Channel estimation and adaptive power allocation for performance and capacity improvement of multiple-antenna OFDM systems", *Wireless Communications, 2001.(SPAWC'01). 2001 IEEE Third Workshop on Signal Processing Advances*, pp. 82-85, 2001.

[17]. Quoc NH, Larsson EG, Marzetta TL, "Aspects of favorable propagation in massive-MIMO." *In: Proc. 2014 Proceedings of the 22nd European Signal Processing Conference (EUSIPCO)*, pp:76-80, September 2014.

[18]. Cho, YS and Kim, J and Yang, WY and Kang, CG, "MIMO-OFDM Wireless Communication Technology with MATLAB",*Beijing: Publishing House of Electronics Industry*, 2013.

[19]. Kwon, Seok-Chul and Stuber, Gordon L, "Geometrical theory of channel depolarization",*IEEE Transactions on Vehicular Technology*, Vol.60,No.8, pp.3542-3556, 2011.

[20]. Jiang, Lei and Thiele, Lars and Jungnickel, Volker, "On the modelling of polarized MIMO channel",*Proc. Europ. Wireless*, pp. 1-4, 2007.

[21]. Yejun He, Xudong Cheng, and Gordon L. Stuber, "On polarization channel modeling",*IEEE Wireless Communications*, Vol.23, No.1, pp.80-86, February 2016 .

[22]. M. Coldrey, "Modeling and Capacity of Polarized MIMO Channels", *VTC Spring 2008-IEEE Vehicular Technology Conference*, pp. 440-444, May 2008 .

[23]. A. Habib, B. Krasniqi, and M. Rupp, "Convex Optimization for Receive Antenna Selection in Multi-Polarized MIMO Transmissions", *Proc. IEEE Sys., Signals and Image Processing Conf*,pp.269-75, April 2012.

[24]. Jeon, KwangHyun and Hui, Bing and Chang, KyungHi and Park, HyeongSook and Park, YounOk, "SISO Polarized Flat Fading Channel Modeling for Dual-Polarized Antenna Systems",*The International Conference on Information Network*,pp.368-373, Feb.2012.

[25]. Ma, You and Zheng, Zhi and Zhou, Yu-long, "Characteristics of MIMO channel in consideration of polarization",*2009 5th International Conference on Wireless Communications, Networking and Mobile Computing*, pp.1-3, 2009.

[26]. Park, Jaehyun and Clerckx, Bruno,"Multi-user linear precoding for multi-polarized massive-MIMO system under imperfect CSIT",*IEEE Transactions on Wireless Communications*, Vol.14, No.5, pp. 2532-2547, 2015.

[27]. Yang, Shaoshi and Hanzo, Lajos, "Fifty years of MIMO detection: The road to large-scale MIMOs", *IEEE Communications Surveys Tutorials*, Vol.17, No.4, pp. 1941-1988, 2015.

[28]. Chockalingam, A and Rajan, B Sundar, "Large MIMO systems",*Cambridge University Press*, pp. 46 2014.

[29]. Li, Jinxing and Zhao, Youping and Tan, Zhenhui, "Indoor channel measurements and analysis of a large-scale antenna system at 5.6 GHz",*2014 IEEE/CIC International Conference on Communications in China (ICCC)*, pp.281-285, 2014.

[30]. Fredrik Rusek, Daniel Persson, Buon Kiong Lau, Erik G. Larsson, Thomas L. Marzetta, Ove Edfors, and Fredrik Tufvesson, "Scaling up MIMO: Opportunities and challenges with very large arrays",*IEEE SIGNAL PROCESSING MAGAZINE*, 2013.

[31]. Gao, Xiang and Edfors, Ove and Rusek, Fredrik and Tufvesson, Fredrik,"Linear Pre-Coding Performance in Measured Very-Large MIMO Channels",*IEEE Vehicular Technology Conference(VTC Fall)*, pp.1-5, 2011.

[32]. Soma, Pitchaiah and Baum, Daniel S and Erceg, Vinko and Krishnamoorthy, Rajeev and Paulraj, AJ, "Analysis and modeling of multiple-input multiple-output (MIMO) radio channel based on outdoor measurements conducted at 2.5 GHz for fixed BWA applications",*2002 IEEE International Conference on Communications. Conference Proceedings. ICC 2002 (Cat. No. 02CH37333)*, Vol.1, pp.272-276, 2002.

[33]. Younes Djemamar, Saida Ibnyaich and Abdelouhab Zeroual,"Space-time Block Coding Techniques for Minimizing BER for MIMO 2×2 System in Rayleigh Fading Channel",*Journal of Engineering Technology*, pp.18-30, 2019.

[34]. Md. Abdul Latif Sarker, K.M. Cho, Tae Chol Shin, Moon Ho Lee,"A Unified Linear Precoding Design for Multiuser MIMO Systems", *Journal of Engineering Technology*, pp.273-279, 2017.

[35]. Riadi A., Boulouird M., Hassani M M. (2020) Least Squares Channel Estimation of an OFDM Massive MIMO System for 5G Wireless Communications. In: Bouhlel M., Rovetta S. (eds) Proceedings of the 8th International Conference on Sciences of Electronics, Technologies of Information and Telecommunications (SETIT'18), Vol.2. SETIT 2018. Smart Innovation, Systems and Technologies, vol 146. Springer, Cham.

[36]. Abdelhamid Riadi, Mohamed Boulouird and Moha M'Rabet Hassani, "ZF/MMSE and OSIC Detectors for UpLink OFDM Massive MIMO systems", 2019 IEEE Jordan International Joint Conference on Electrical Engineering and Information Technology (JEEIT), p.p. 767 – 772, 9-11 April 2019, Amman, Jordan, 2019.

[37]. Abdelhamid Riadi, Mohamed Boulouird, and Moha M'Rabet Hassani, "Performance of Massive-MIMO OFDM system with M-QAM Modulation based on LS Channel Estimation", 3rd International Conference on Advanced Systems and Emergent Technologies (IC ASET'2019), Hammamet, Tunisia, 19-22 March 2019.

[38]. Mohamed Boulouird, Abdelhamid Riadi, and Moha M'Rabet Hassani, "Pilot contamination in multi-cell Massive-MIMO systems in 5G wireless communications". 2017 International Conference on Electrical and Information Technologies (ICEIT) - Rabat, Morocco, 15-18 Nov. 2017.